

# Matrine Inhibits Breast Cancer Cell Proliferation and Epithelial-Mesenchymal Transition Through Regulating the LINC01116/miR-9-5p/ITGB1 Axis

Lili Ren<sup>1</sup>, Ziru Fang<sup>2</sup>, Jiaojiao Xu<sup>2</sup>, Xiaoxiao Wu<sup>3</sup>, Yongjun Zhang<sup>1</sup>, Hu Cai<sup>1</sup>, Zhicun Han<sup>4</sup>

<sup>1</sup>Department of Integration of Traditional Chinese and Western Medicine, Zhejiang Cancer Hospital, Hangzhou Institute of Medicine (HIM), Chinese Academy of Medical Sciences, Hangzhou, Zhejiang 310022, China

<sup>2</sup>Department of Medical Oncology, Zhejiang Cancer Hospital, Hangzhou Institute of Medicine (HIM), Chinese Academy of Sciences, Hangzhou, Zhejiang 310022, China

<sup>3</sup>Department of Pathology, Zhejiang Cancer Hospital, Hangzhou Institute of Medicine (HIM), Chinese Academy of Sciences, Hangzhou, Zhejiang 310022, China

<sup>4</sup>Department of Acupuncture, Tongde Hospital of Zhejiang Province, Hangzhou, Zhejiang 310022, China

**Background:** Breast cancer (BC) is the most prevalent solid cancer affecting women's health globally. Matrine (MAT), a traditional Chinese herb, has exhibited antitumor effects against BC. However, its mechanism of action, particularly whether it involves the control of cell proliferation and epithelial-mesenchymal transition (EMT), remains unknown.

**Aims:** To explore MAT's role in BC and its regulatory mechanisms, as well as to identify targets for the development of novel medicines and improvement of BC treatment modalities.

**Study Design:** Experimental study.

**Methods:** The UALCAN and Lnc2Cancer 3.0 databases were used to predict the expression of LINC01116 in BC. The BC cells (MDA-MB-231 and MCF-7) were treated with various concentrations of MAT, and the optimal dose and timing of MAT action were determined using CCK-8 and quantitative real-time polymerase chain reaction assays. Functional assays such as CCK-8, EdU, Transwell, Western blot, and flow cytometry assays were performed on the BC cells, and the impacts of LINC01116, miR-9-5p, and

ITGB1 expression levels on MAT's mechanism of action were assessed. The association between LINC01116, miR-9-5p, and ITGB1 was evaluated using dual luciferase and RNA immunoprecipitation assays. Furthermore, the size and weight of the subcutaneous tumors in mice model were assessed. The effect of LINC01116 overexpression on the in vivo action of MAT and histopathological staining (TUNEL immunofluorescence, hematoxylin & eosin staining, immunohistochemistry staining for Ki67 and Bax) were also assessed.

**Results:** The optimal dose and duration of MAT administration were 8 μm and 24 h, respectively. MAT effectively inhibited BC cell proliferation, EMT progression, and biological functions, while promoting BC cell apoptosis. The animal model experiments also demonstrated that MAT inhibited BC tumor growth in vivo. Furthermore, MAT inhibited LINC01116, which acted as a sponge for miR-9-5p, increasing the ITGB1 level.

**Conclusion:** MAT suppresses BC cell and EMT proliferation via the LINC01116/miR-9-5p/ITGB1 pathway. Thus, MAT may be a promising target for adjuvant anti-BC therapy.

## INTRODUCTION

In 2020, the global incidence rate of breast cancer (BC) was approximately 2.3 million, with a 6.9% fatality rate.<sup>1,2</sup> In recent years, with industrialization, urbanization, and changes in lifestyle, the incidence of BC has increased annually, and the affected population has become younger.<sup>3,4</sup> Although therapeutic drugs and surgical

modalities for BC are constantly being developed, the recurrence and mortality rates for BC continue to rise. Thus, identifying more precise drug targets or combining modalities has become critical for the eradication of BC and prevention of recurrence. Unlike typical anticancer medications, Chinese medicine has fewer side effects and focuses on balancing the yin and yang, which has some advantages over contemporary medicine.<sup>5-7</sup>



**Corresponding author:** Zhicun Han, Department of Acupuncture, Tongde Hospital of Zhejiang Province, Hangzhou, Zhejiang 310022, China

**e-mail:** hanzc1978@163.com

**Received:** September 14, 2024 **Accepted:** December 10, 2024 **Available Online Date:** January 02, 2025 • **DOI:** 10.4274/balkanmedj.galenos.2024.2024-8-49

Available at [www.balkanmedicaljournal.org](http://www.balkanmedicaljournal.org)

**ORCID iDs of the authors:** L.R. 0000-0003-3766-2350; Z.F. 0000-0002-9858-5742; J.X. 0000-0001-5436-3059; X.W. 0009-0000-7455-504X; Y.Z. 0000-0002-2326-7870; H.C. 0000-0002-9178-5960; Z.H. 0000-0003-0507-0203.

**Cite this article as:** Ren L, Fang Z, Xu J, Wu X, Zhang Y, Cai H, Han Z. Matrine Inhibits Breast Cancer Cell Proliferation and Epithelial-Mesenchymal Transition Through Regulating the LINC01116/miR-9-5p/ITGB1 Axis. Balkan Med J; 2025; 42(1):54-65.

Copyright@Author(s) - Available online at <http://balkanmedicaljournal.org>

With the continued development and progress of Chinese medicine, certain studies have used Chinese herbs in the treatment of BC.<sup>8,9</sup> Exploring the active ingredients in Chinese herbs is a key measure to improving the curative rate, reducing the recurrence of BC, and directing primary studies toward Chinese herbs for BC prevention and treatment. The active compounds in Chinese herbs can suppress the development of BC via several pathways and targets, thereby reducing metastasis, recurrence rates, and side effects associated with treatment.<sup>10,11</sup> Matrine (MAT) is an active ingredient derived from the root of the traditional Chinese medicine *Sophora flavescens radix*. It is a tetracyclic quinolizidine alkaloid that exhibits numerous physiological and pharmacological properties, including antiinflammatory, antimicrobial, antioxidant, lipid-lowering, and antitumor properties.<sup>12,13</sup> MAT has exhibited anticancer properties in several cancer types, including lung,<sup>14</sup> liver,<sup>15</sup> gastric,<sup>16</sup> pancreatic,<sup>17</sup> and gynecological malignancies (cervical, ovarian, and breast).<sup>18-20</sup> MAT can exert antitumor effects via various pathways, including cell growth, autophagy induction, cell migration and invasion inhibition, tumor neoangiogenesis inhibition, reversal of multidrug resistance in tumor cells, and body immunity regulation.<sup>21,22</sup> However, its principal mode of action is to inhibit tumor-related signaling pathways, resulting in a substantial anticancer efficacy.<sup>23</sup> Although MAT is effective in treating BC,<sup>18</sup> its mechanism of action requires further exploration.

The occurrence, development, invasion, and metastasis of BC are associated with epithelial-mesenchymal transition (EMT). During the progression of BC, EMT in tumor cells reduces intercellular junctions, promotes individual tumor cell detachment from the carcinoma in situ, and promotes the acquisition of mesenchymal properties. These allow the cells to migrate to and invade the periphery, enter the circulatory system, and eventually disseminate to distant organs.<sup>24-26</sup> EMT is associated with the activation of various signaling pathways. MAT can prevent EMT in gallbladder cancer by modulating the PI3K/AKT pathway.<sup>27</sup> It also hinders EMT in pancreatic cancer cells via the ROS/NF-κB/MMPs pathway.<sup>28</sup> However, studies on MAT regulating EMT in BC are limited, and the underlying mechanisms need to be further explored.

MAT can exert anticancer effects via the regulation of lncRNA-miRNA interactions, which play a role in cancer etiology via multiple signaling pathways. MAT has exhibited anticancer benefits against acute myeloid leukemia by inhibiting the JAK/STAT pathway, which is regulated by lncRNA LINC01116/miR-592.<sup>29</sup> The lncRNA NUTM2A-AS1/microRNA-613 plays a role in MAT's mechanism of action for suppressing gastric cancer.<sup>30</sup> LINC01116 is located in the 2q31.1 region of the chromosome, with a length of roughly 1050 bp. Its abnormal expression has been related with several malignancies, and it plays a role in encouraging the development of cancer cells.<sup>31</sup> Numerous studies have demonstrated that RNA01116 can affect EMT progression in tumor cells, resulting in tumor progression and a bad prognosis. However, it is uncertain whether MAT can regulate LINC01116,<sup>32,33</sup> and currently, there are no reports of an association between LINC01116 and BC.

Based on the research background, we aimed to investigate the effects of MAT on LINC01116 expression in BC cells and a nude

mice transplantation tumor model. Using cellular experiments and an animal model, the genes targeted by LINC01116 and potential regulatory pathways were screened, and the effects of these pathways on MAT-regulated cell proliferation, EMT, and tumor development were analyzed. The goal of the study was to explore MAT's role in BC and its regulatory mechanisms, as well as to generate ideas for developing MAT-targeted medicines and improving BC therapy techniques.

## MATERIALS AND METHODS

This study was approved by the Medical Ethics Committee of Zhejiang Cancer Hospital, Hangzhou Institute of Medicine, Chinese Academy of Sciences (approval number: YL-20231023, date: 23.10.2023).

### Bioinformatics analysis

The level of LINC01116 in BC tissues was evaluated using the online databases UALCAN (<https://ualcan.path.uab.edu/>) and Lnc2Cancer 3.0 (<http://bio-bigdata.hrbmu.edu.cn/lnc2cancer/>). The ENCORI (<https://rnasysu.com/encori/>) was used to predict the binding sites between LINC01116, miR-9-5p, and ITGB1.

### Cell cultivation

The Cell Bank of the Chinese Academy of Sciences (Shanghai, China) provided MCF-10A cells and BC cells (MDA-MB-231 and MCF-7). All cells were grown in a RPMI-1640 medium (ORCPM0110B; ORICells, Shanghai, China), which was supplemented with 100 U/ml of a penicillin-streptomycin solution (C0222; Beyotime, Shanghai, China) and 10% fetal bovine serum [(FBS); C0235]. All cells were incubated in a saturated humidity incubator at 37 °C, with 5% CO<sub>2</sub>.

### Cell transfection

RiboBio (Guangzhou, China) provided LINC01116 overexpression (LINC01116) and the negative control (vector), miR-9-5p overexpression and the negative control (miR-NC), and ITGB1 knockdown (si-ITGB1) and the negative control (si-NC). The cells were transfected using the Lipofectamine 3000 (L3000001; Invitrogen, Austin, TX, USA) protocols, with all transfections lasting 48 h.

### CCK-8 assay

The BC cells (MDA-MB-231 and MCF-7) were digested with trypsin, centrifuged, and counted. The cells were inoculated into 96-well plates (1 × 10<sup>4</sup> cells/well), and 200 μl of culture medium was added to each well. The BC cells were treated with 2 μm, 4 μm, and 8 μm of MAT, and subsequently incubated at 37 °C with 5% CO<sub>2</sub> incubator. During each time period, 20 μl of CCK-8 reagent was added, and the cells were incubated for 2 h. The proliferative vitality of the cells in each well was evaluated using an enzyme marker (OD at 450 nm).

Based on the OD value, the best dose of MAT was 8 μm, which was utilized to treat the transfected BC cells in all subsequent studies. The remaining processes were the same as those described above.

### **EdU detection**

The BC cells were inoculated in 24-well plates ( $2 \times 10^4$  cells/well), and 8 µm of MAT was added to each well. After the cells were cultivated for 24 h, the culture media were discarded. Subsequently, the cells were rinsed with PBS and treated with 10 µm of EdU staining solution for 1 h without light. Thereafter, the cells were rinsed with PBS and fixed and permeabilized using 4% paraformaldehyde and 0.3% triton X-100, respectively. Subsequently, the cells were incubated with the click reaction solution for 30 min at room temperature without light. Thereafter, the nuclei were stained with DAPI for 10 min, and the slides were sealed. The slides were examined for positively stained cells using a fluorescence microscope, and photographs were obtained.

### **Transwell detection**

Transwell inserts were inserted into 24-well plates in which 50 µl of pre-cooled matrix gel (Matrigel) had been added to the chambers to test for invasiveness. The upper chamber was filled with 100 µl of  $1 \times 10^5$ /ml cell suspension and 8 µm MAT, and the lower chamber was filled with 500 µl of RPMI-1640 media containing 10% FBS. The plates were incubated at 37 °C and 5% CO<sub>2</sub> for 24 h. Thereafter, the cells in the lower chamber were fixed with 4% paraformaldehyde and stained with 0.1% crystal violet. Subsequently, the plates were rinsed with PBS and air-dried. Thereafter, a high magnification microscope was used to identify the number of cells that had migrated and invaded the lower chamber.

### **Flow cytometry**

Apoptosis was detected using the Annexin V-FITC/PI Double Labeling Staining Kit (40302ES50; Yeasen, Shanghai, China). The cells were treated with 8 µm of MAT for 24 h, and subsequently washed twice with pre-cooled PBS. Thereafter, the cells were collected, centrifuged, and resuspended in 100 µl of binding buffer, 5 µl of annexin V-FITC, and 10 µl of PI. The reagents were allowed to react for 15 min at 25 °C without light. Thereafter, the binding buffer was added, and a flow cytometer (2010284AA; Agilent, Santa Clara, CA, USA) was used to detect and quantify the rate of apoptosis.

### **Dual luciferase assay**

LINC01116 and ITGB1 3'UTR sequences with wild-type (WT) or mutant (MUT) miR-9-5p binding sites were introduced into the pmirGLO vector (Promega, WI, USA) to generate the following luciferase reporter plasmids: WT-LINC01116, MUT-LINC01116, WT-ITGB1, and MUT-ITGB1. The MDA-MB-231 and MCF-7 cells were transfected with the aforementioned plasmids, as well as miR-9-5p or miR-NC, using Lipofectamine 3000 (L3000001; Invitrogen). The luciferase activity after 48 h of cotransfection was detected using a dual luciferase reporter assay kit (RG027; Beyotime).

### **RNA immunoprecipitation assay**

To verify the binding of LINC01116 and miR-9-5p, the RNA immunoprecipitation (RIP) test was performed (JKR23003 RIP kit; Gene Create, Wuhan, China). The BC cells were lysed with RIP lysate. Thereafter, 100 µl of the whole cell extracts were treated with magnetic beads bearing AGO2-conjugated antibodies for 2 h

at room temperature. Immunoglobulin G (IgG) antibodies served as a control. Thereafter, the samples were washed with the RIP wash buffer and processed with proteinase K for 30 min at 55 °C to extract RNA-protein complexes from the magnetic beads. Subsequently, the immunoprecipitated RNA was extracted using Trizol, and quantitative polymerase chain reaction (qPCR) was performed to determine the enrichment of LINC01116 and miR-9-5p.

### **In vivo experiment**

An in vivo model was developed using 4-week-old female BALB/c nude mice. The animals were administered subcutaneous injections of MDA-MB-231 cells that were transfected with a vector or LINC01116 ( $2 \times 10^6$  cells/mice). When the tumor volume was  $\geq 150$  mm<sup>3</sup><sup>34</sup> the nude mice were randomly separated into the following three groups (n = 5 each): control (vector), MAT administration (vector + MAT), and LINC01116 overexpression + MAT administration (LINC01116 + MAT). MAT was administered at a dose of 100 mg/kg/d. Vernier calipers were used to quantify the tumor volume (1/2 × length × width<sup>2</sup>) every 7 days, and photographs were obtained. After 21 days (day 28) of continuous intraperitoneal injection, the nude mice were killed, and the tumors were isolated and weighed.

### **TUNEL immunofluorescence assay**

Apoptosis in the tumor tissues was measured using a TUNEL kit (C1091; Beyotime, Shanghai, China). The test was performed according to the manufacturer's instructions. Tumor tissues from the mice were fixed with 4% paraformaldehyde, hydrated, embedded in paraffin, and cut into 4 µm slices. The tissue sections were deparaffinized with xylene and dehydrated using an ethanol gradient. The section was rinsed with PBS before each of the following steps: addition of 20 µg/ml of DNase-free proteinase K solution and incubation at 25 °C to allow reagents to enter the nucleus. Subsequently, the tissues were soaked in 3% H<sub>2</sub>O<sub>2</sub> for 15 min to deactivate the endogenous peroxidase in the slices. Thereafter, the slices were stained with 50 µl of the TUNEL reaction mix (60 min at 37 °C), followed by the DAPI staining solution (5 min at room temperature) under light protection. Subsequently, the sections were blocked with an anti-fluorescent burst sealing solution and tested for TUNEL positivity.

### **Hematoxylin & eosin staining**

The paraffinized tumor sections were deparaffinized using xylene and rehydrated using an alcohol gradient. Thereafter, the sections were stained with hematoxylin for 15 min, differentiated with 1% acidic alcohol (containing 70% hydrochloric acid) for 30 seconds, and rinsed under running water. Subsequently, the section was stained with 0.5% eosin for 3 min. Thereafter, the slices were dehydrated using an alcohol gradient, treated with xylene transparency, and sealed with a neutral gum (G8590; Solarbio). Finally, the tumor morphology was examined under a microscope.

### **Immunohistochemistry**

The tissue sections were subjected to ethanol gradient hydration and citrate antigen repair (C1032; Solarbio). Ki67 (ab232784) and Bax (ab32503) primary antibodies were added to the section after

the addition of an avidin/biotin blocking buffer (C-0005; HaoRan Biotech, Shanghai, China) at 25 °C. Subsequently, the sections were incubated overnight at 4 °C. After incubation, the sections were washed, and the appropriate secondary antibody (ab150077) was added. Thereafter, the sections were incubated for 1 h at 25 °C. Subsequently, the sections were restained with streptavidin-horseradish peroxidase and hematoxylin (C0107; Beyotime, Shanghai, China). Finally, the sections were dehydrated using an ethanol concentration gradient, permeabilized using xylene, sealed with a neutral gum, and evaluated using a microscope. The microscopic appearance was photographed.

#### **qRT-PCR assay**

Total RNA was isolated from the BC cells and mice model tumors using Trizol (DP424; Tiangen, Beijing, China). The RNA was reverse transcribed to cDNA using the Prime Script RT reagent Kit (RR047 A; Takara, Tokyo, Japan). Thereafter, quantitative real-time polymerase chain reaction (qRT-PCR) was performed (ABI PRISM 7300). The  $2^{-\Delta\Delta C_t}$  technique was used to calculate the relative expression levels of LINC01116 and miR-9-5p, and their data were normalized using β-actin and U6, respectively. The following primers were used:

- LINC01116: F, 5'-ATTGACCCTTCGGACAGCAG-3'; R, 5'-GGGAATCGGCAGGAAATGA-3'.
- β-actin: F, 5'-ATCACTATTGGCAACGAGCG-3'; R, 5'-ACTCATCGTACTCCTGCTTG-3'.
- miR-9-5p: F, 5'-AAGCAGAACCGAAAGAAAAA-3'; R, 5'-AGTCAGGGTCCGAGGTATT-3'.
- U6: F, 5'-CTCGCTCGGCAGCACA-3'; R, 5'-AACGCTTCACGAATTGCGT-3'.

#### **Western blot analysis**

The BC cells and tumor tissue samples were lysed using a lysis buffer (20101ES60; Yeasen, Shanghai, China), and the proteins were isolated using 10% SDS-PAGE. The protein samples were transferred to PVDF membranes, and the membranes were treated with TBST buffer containing 5% skimmed milk for 1 h at 25 °C. Thereafter, the membranes were incubated overnight at 4 °C with the primary antibody. Subsequently, the membranes were incubated with the secondary antibody for 1 h at 25 °C. The immunoblots were observed using enhanced chemiluminescence. A chemiluminescence image analysis system (5200; Tanon, Shanghai, China) and ImageJ (version 1.8.0) were used to capture the protein bands and analyze the grayscale values, respectively.

The primary antibodies used were rabbit anti-E-cadherin (ab314063), Snail (ab180714), Vimentin (ab92547), ITGB1 (ab179471), and the endogenous reference protein β-actin (ab8227). The secondary antibody used was sheep anti-rabbit IgG (ab6721). All the additional antibodies were acquired from Abcam and used at the appropriate concentrations.

#### **Statistical analysis**

All data were analyzed using SPSS (version 26.0), and the figures were created using GraphPad Prism (version 9.0). The t-test was used to compare samples from two groups, whereas ANOVA was used

to compare samples from several groups. Subsequently, the post-hoc Tukey test was used. Data are presented as mean ± standard deviation. Statistical significance was set at  $p < 0.05$ .

## **RESULTS**

### **LINC01116 was significantly expressed in BC cells**

An online analysis using the UALCAN and the Lnc2Cancer 3.0 databases revealed that the expression level of LINC01116 was considerably greater in the BC cells than in the normal samples (Figure 1a, b). Validation by qRT-PCR using normal human mammary epithelial cells MCF-10A and human BC cells (MCF-7 and MDA-MB-231 cells) revealed that LINC01116 expression had significantly increased in the BC cells (Figure 1c). This implies that LINC01116 may play a role in BC deterioration. The CCK-8 assay to examine the effect of MAT on the proliferative viability of BC cells and screen for the optimal concentration of MAT for its activity. The MCF-7 and MDA-MB-231 cells were treated with 2, 4, and 8 μm of MAT for 0, 24, 48, and 72 h. The CCK-8 assay revealed that cell concentration increased in a time-dependent manner in all groups. Furthermore, MAT suppressed the proliferation of MCF-7 and MDA-MB-231 cells in a concentration-dependent manner, with 8 μm of MAT exhibiting the largest inhibitory effect on both cell lines (Figure 1d, e). The qRT-PCR assay revealed that the levels of LINC01116 in BC cells were lower than that in the control group after exposure to 8 μm of MAT for 24, 48, and 72 h ( $p < 0.001$ , Figure 1f, g). Therefore, except for the CCK-8 assay, our subsequent experiments were performed with 8 μm MAT for 24 h.

### **LINC01116 overexpression reduced the inhibitory impact of MAT on cancer progression**

After transfecting the two MAT-treated BC cell lines with the LINC01116 overexpression vector, the qRT-PCR revealed overexpression of LINC01116 (Figure 2a). The MCF-7 and MDA-MB-231 cells in the vector + MAT group demonstrated low OD450 values (Figure 2b, c), EdU-positive cells, reduction in the number of cells migrating to and invading the lower compartment (Figure 2d-i), increased expression of EMT-related protein E-cadherin, decreased expression of Snail and vimentin (Figure 2j-l), and an increased apoptosis rate (Figure 2m, n). These findings indicate that MAT could effectively inhibit the malignant biology. Furthermore, LINC01116 overexpression partially reversed MAT's inhibitory effect on the malignant behavior of BC cells, promoting their malignant behavior while inhibiting their death. Thus, MAT may slow cancer growth by modulating LINC01116 expression.

### **LINC01116 functioned as a sponge for miR-9-5p in the BC cells**

Through screening, we discovered a potential binding site (UGGUUUC) between LINC01116 3'UTR and miR-9-5p (Figure 3a). After verification of miR-9-5p overexpression efficiency by qRT-PCR (Figure 3b), we found that although the miR-9-5p overexpression significantly reduced the luciferase activity of WT-LINC01116, it did not affect the MUT-LINC01116 luciferase activity (Figure 3c).

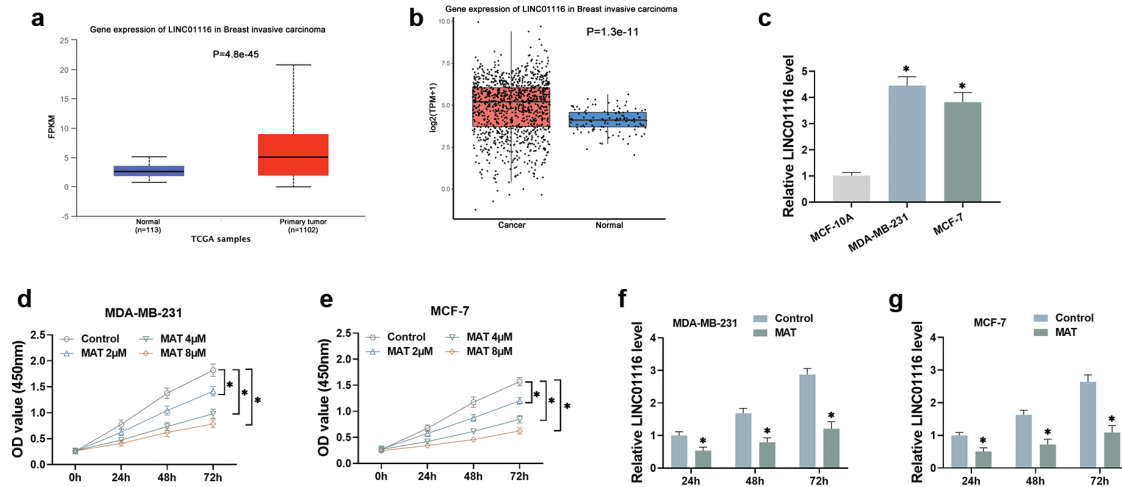


**FIG. 1.** MAT inhibits LINC01116, a highly expressed protein in BC (\*indicates  $p < 0.05$ ). (a) The UALCAN database projected the expression levels of LINC01116 in BC tissues. (b) The expression of LINC01116 in BC tissues was predicted using the Lnc2Cancer 3.0 database. (c) The expression of LINC01116 in human normal breast epithelial cells MCF-10A and BC cells (MCF-7 and MDA-MB-231) was determined using qRT-PCR. (d, e) MCF-7 and MDA-MB-231 cells were treated with 2, 4, and 8  $\mu$ M of MAT, respectively. Cell proliferation changes were observed by CCK-8 after different times of cell culture, resulting in the optimal treatment dose of MAT (8  $\mu$ M). (f, g) qRT-PCR results showed that the expression levels of LINC01116 in two types of BC cells were considerably reduced after 24 h, 48 h, and 72 h of treatment with 8  $\mu$ M MAT, hence the treatment time was decided to be 24 h. The findings revealed that the expression levels of LINC01116 were considerably reduced after 24 h, 48 h and 72 h of treatment with 8  $\mu$ M MAT.

BC, breast cancer; MAT, matrine; qRT-PCR, quantitative real-time polymerase chain reaction.

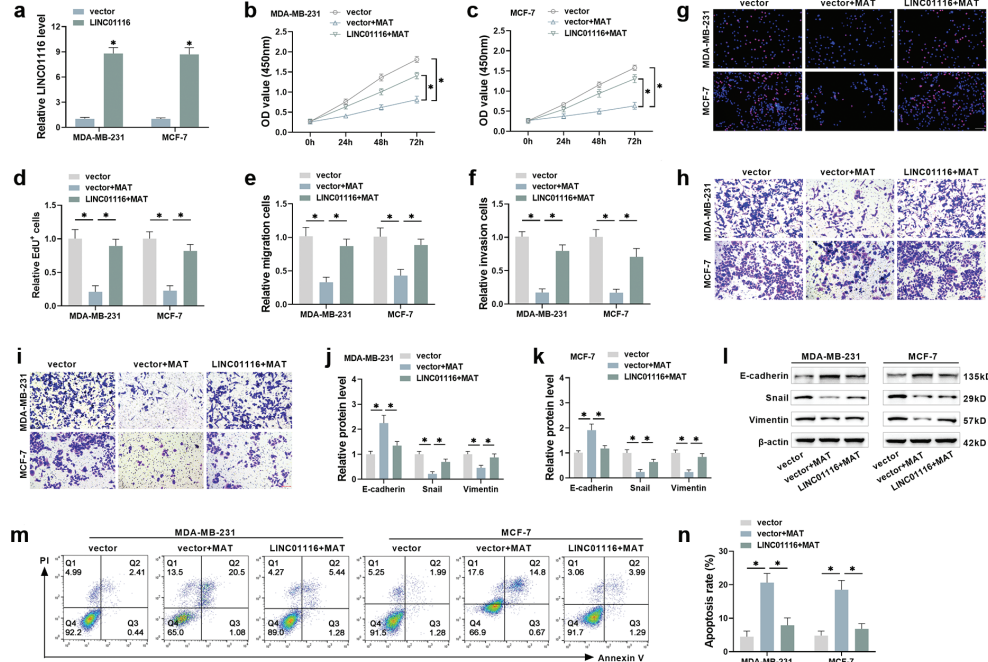


**FIG. 2.** LINC01116 overexpression reduces the inhibitory influence of MAT on BC development (\*indicates  $p < 0.05$ ). (a) The LINC01116 overexpression vector was transfected into two types of BC cells, and the vector's transfection efficiency was validated by qRT-PCR. (b, c) CCK-8 detected alterations in the proliferation of BC cells under various treatment settings. (d, g) EdU measured the proportion of positive cells in BC cells to quantify their proliferation. (e, h) Transwell detection of BC cell migration into the lower chamber. (f, i) Transwell detection of the amount of BC cells invading the lower compartment. (j, l) Western blot analysis of EMT-related proteins E-cadherin, snail, and vimentin in BC cells. (m, n) Flow assay for detecting apoptosis levels in BC cells.

BC, breast cancer; MAT, matrine; qRT-PCR, quantitative real-time polymerase chain reaction; EMT, epithelial-mesenchymal transition.

Furthermore, the enrichment of LINC01116 in BC cells significantly increased following miR-9-5p overexpression ( $p < 0.0001$ , Figure 3d), indicating that LINC01116 binds to miR-9-5p. The qRT-PCR revealed that miR-9-5p levels significantly reduced following LINC01116 overexpression ( $p < 0.0005$ ) and that miR-9-5p expression was significantly lower in BC cells than in MCF-10A cells ( $p < 0.001$ ) (Figure 3e, f). These demonstrate that LINC01116 binds to miR-9-5p. Our findings imply that LINC01116 serves as a sponge for miR-9-5p in BC cells, and it promotes BC by suppressing miR-9-5p production.

### Overexpression of miR-9-5p reversed LINC01116's inhibitory effect on MAT activity

We investigated whether MAT can alter BC cell function by controlling the expression levels of LINC01116 and miR-9-5p, which were confirmed by rescue experiments. The experiments were divided into the following four groups: control group (vector + miR-NC), MAT-treated group (vector + miR-NC + MAT), LINC01116 overexpression in MAT-treated group (LINC01116 + miR-NC + MAT), and LINC01116 and miR-9-5p overexpression in MAT-treated group (LINC01116 + miR-9-5p + MAT). LINC01116 overexpression significantly reduced MAT's inhibitory impact on cell biological behaviors. In contrast to the LINC01116 + miR-NC + MAT group, the LINC01116 + miR-9-5p + MAT group exhibited suppression of the malignant behavior of the two BC cell lines. In the LINC01116 + miR-9-5p + MAT group, the cell proliferation viability was significantly reduced ( $p < 0.0001$ , Figure 4a, b), the cellular EdU positivity rate was elevated (Figure 4c, d), the number of cells migrating to and invading the lower chamber was significantly reduced ( $p < 0.0001$ , Figure 4e-h), the Snail and

vimentin levels were significantly reduced ( $p < 0.05$ , Figure 4i, j), and the apoptosis rate was significantly higher ( $p < 0.005$ , Figure 4k, l). Thus, miR-9-5p overexpression substantially reversed the inhibitory impact of LINC01116 on MAT function, indicating that MAT inhibits BC via the LINC01116/miR-9-5p axis.

### LINC01116 enhanced ITGB1 expression by acting as a sponge for miR-9-5p

miRNAs serve important biological activities by controlling the expression levels of downstream genes. Hence, it is critical to investigate miRNA functional mechanisms, including the identification of significant target genes and regulatory relevance. Although our findings indicate that MAT inhibits BC cell proliferation and EMT via the LINC01116/miR-9-5p axis, it remains unclear which target gene miR-9-5p regulates BC cell activity. Bioinformatics analysis by the ENCORI database predicted that the miR-9-5p's downstream target gene was ITGB1 (Figure 5a). WT-ITGB1 and MUT-ITGB1 were co-transfected with the miR-9-5p overexpression vector and the control miR-NC vector, respectively, into the two BC cell lines. The miR-9-5p overexpression strongly suppressed the luciferase activity of WT-ITGB1 ( $p = 0.0001$  and  $p = 0.0003$ , respectively; Figure 5b). This indicated that miR-9-5p specifically binds to ITGB1. Western blot analysis revealed that ITGB1 expression significantly reduced following miR-9-5p overexpression in the BC cells ( $p < 0.0001$ , Figure 5c). However, ITGB1 expression was higher in the BC cells than in MCF-10A cells (Figure 5d). We hypothesized that the downregulation of LINC01116 could promote miR-9-5p expression, which in turn may inhibit ITGB1 production and prevent BC progression. This conclusion was supported by the fact that the

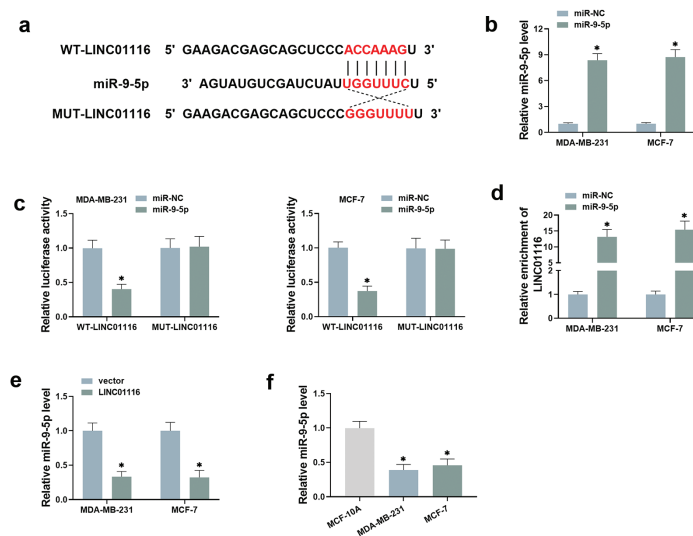


**FIG. 3.** LINC01116 acts as a sponge for miR-9-5p in BC cells (\*indicates  $p < 0.05$ ). (a) The ENCORI database predicted LINC01116's binding location to miR-9-5p. (b) The miR-9-5p overexpression plasmid was transfected into two types of BC cells, and cell transfection efficiency was assessed using qRT-PCR. (c) WT-LINC01116 and MUT-LINC01116 luciferase reporter plasmids were co-transfected with miR-9-5p overexpression vector and control miR-NC vector into two types of BC cells, respectively, and the cells' luciferase activity was measured. (d) The RIP assay was used to determine the enrichment of LINC01116 with miR-9-5p in two types of BC cells. (e, f) The LINC01116 overexpression vector was transfected into two types of BC cells, and miR-9-5p expression alterations were identified using qRT-PCR.

BC, breast cancer; qRT-PCR, quantitative real-time polymerase chain reaction; RIP, RNA immunoprecipitation.

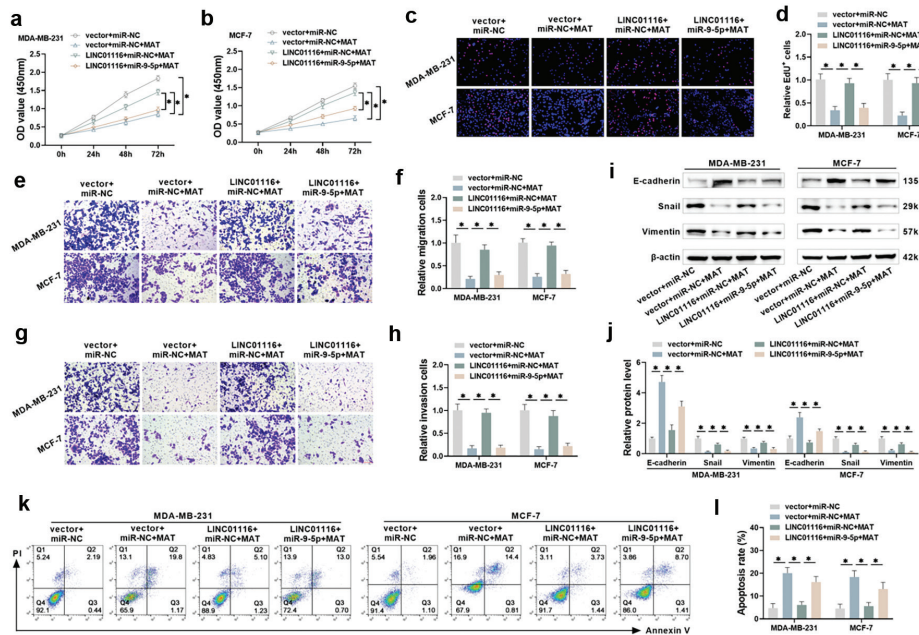


**FIG. 4.** Overexpression of miR-9-5p reduces the attenuating impact of LINC01116 on the suppression of BC development by MAT (\*indicates  $p < 0.05$ ). (a, b) MCF-7 and MDA-MB-231 cells were transfected with miR-9-5p overexpression plasmid and/or LINC01116 overexpression vector. Proliferative changes was measured by CCK-8 after 24, 48, and 72 h of treatment with 8  $\mu$ M MAT. (c, d) EdU measured the proportion of positive cells in two types of BC cells to quantify their proliferation. (e, f) Transwell detection of BC cell migration into the lower chamber. (g, h) Transwell detection of the number of BC cells invading the lower compartment. (i, j) Western blot analysis of EMT-related proteins E-cadherin, snail, and vimentin in two types of BC cells. (k, l) Flow assay for detecting apoptosis levels in two types of BC cells.

BC, breast cancer; MAT, matrine; EMT, epithelial-mesenchymal transition.

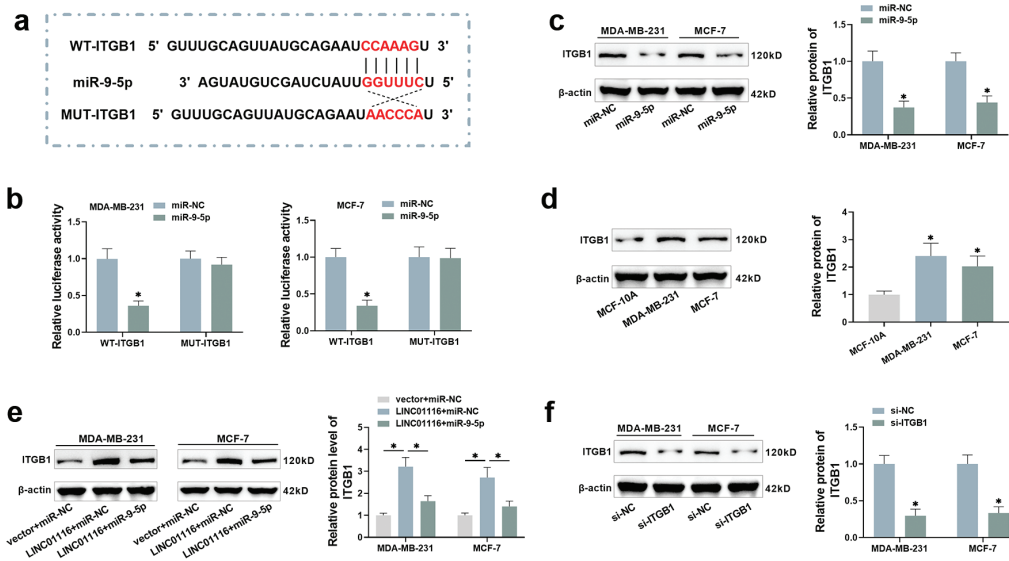


**FIG. 5.** LINC01116 enhances ITGB1 expression through sponge miR-9-5p (\*indicates  $p < 0.05$ ). (a) Predicting miR-9-5p and ITGB1 binding locations using the ENCRI database. (b) WT-ITGB1 and MUT-ITGB1 luciferase reporter plasmids were co-transfected with miR-9-5p overexpression vector and control miR-NC vector into two types of BC cells, respectively, and the cells' luciferase activity was measured. (c) The miR-9-5p overexpression plasmid was transfected into MCF-7 and MDA-MB-231 cells, and changes in ITGB1 expression were observed using Western blotting. (d) Western blot analysis of ITGB1 expression in human normal mammary epithelial cells MCF-10A and BC cells (MCF-7 and MDA-MB-231). (e) The miR-9-5p overexpression plasmid and/or LINC01116 overexpression vector were transfected into two types of BC cells to detect changes in ITGB1 expression. (f) si-ITGB1 was transfected into MCF-7 and MDA-MB-231 cells, and ITGB1 knockdown effectiveness was confirmed by Western blot.

BC, breast cancer.

ITGB1 content in the BC cells was significantly lower when both LINC01116 and miR-9-5p were overexpressed than when LINC01116 was overexpressed alone ( $p < 0.0005$ ; Figure 5e). This demonstrates that LINC01116 upregulates ITGB1 levels by acting as a sponge for miR-9-5p. Furthermore, MAT may function through the LINC01116/miR-9-5p/ITGB1 pathway in BC cells. Subsequently, we transfected si-ITGB1 into two cells to knock down the ITGB1 level (Figure 5f), and we were able to establish the mechanism of action of MAT by rescue tests.

### ITGB1 knockdown rescued the attenuated effect of LINC01116 overexpression on MAT action

Overexpression of LINC01116 considerably reduced the impact of MAT on BC cells. ITGB1 knockdown also reduced the impact of LINC01116 overexpression and partially restored the inhibitory impact of MAT on the proliferative activity of BC cells (Figure 6a, b). Furthermore, there was significant decrease in the proportion of EdU-positive BC cells (Figure 6c, d) and the number of BC cells migrating/invasive into the lower compartment (Figure 6e-h;  $p < 0.0001$ ). In the EMT, there was a significant elevation in the epithelial phenotype-associated protein levels (e-cadherin) and a significant reduction of the mesenchymal phenotype-associated protein (snail and vimentin) levels ( $p < 0.05$ ; Figure 6i, j). Furthermore, there was a significant elevation in the apoptosis rate in the two BC cell lines ( $p < 0.001$ ; Figure 6k, l). Thus, ITGB1 knockdown, similar to miR-9-5p overexpression, reversed the effect of LINC01116 overexpression on MAT action. Furthermore, miR-9-5p targeted and inhibited the

ITGB1 level, indicating that MAT inhibits BC cell proliferation and EMT by regulating the LINC01116/miR-9-5p/ITGB1 pathway.

### LINC01116 overexpression reduced the inhibitory impact of MAT on BC tumor development in vivo

Given the activity of MAT in vitro and the associated pathways, we investigated whether MAT could influence BC tumor formation in vivo. The nude mice transplantation tumor model was created by first subcutaneously injecting MDA-MB-231 cells into nude mice, followed by treatment with MAT (Figure 7a). At the end of the experiment, the nude mice in each group were killed and the size and weight of the subcutaneous tumors were measured. Compared to the vector group, the MAT therapy group exhibited significantly smaller and lighter subcutaneous tumors. However, LINC01116 overexpression encouraged tumor growth, resulting in a considerable increase in both the volume and weight of the tumors (Figure 7b-d).

TUNEL immunofluorescence revealed a considerable reduction in the amount of apoptotic cells following LINC01116 overexpression ( $p < 0.0001$ , Figure 7e, f). Hematoxylin & eosin staining revealed pathological structural abnormalities in the tumor tissues (Figure 7g). The tumors in the vector group revealed a disordered cellular arrangement, increased nuclear-cytoplasmic (N/C) ratio, and tumor tissue infiltration. However, the tumors in the MAT-treated group revealed fewer tumor cells, a fuzzy and sparsely organized morphology, and a decreased N/C ratio. These enhanced the

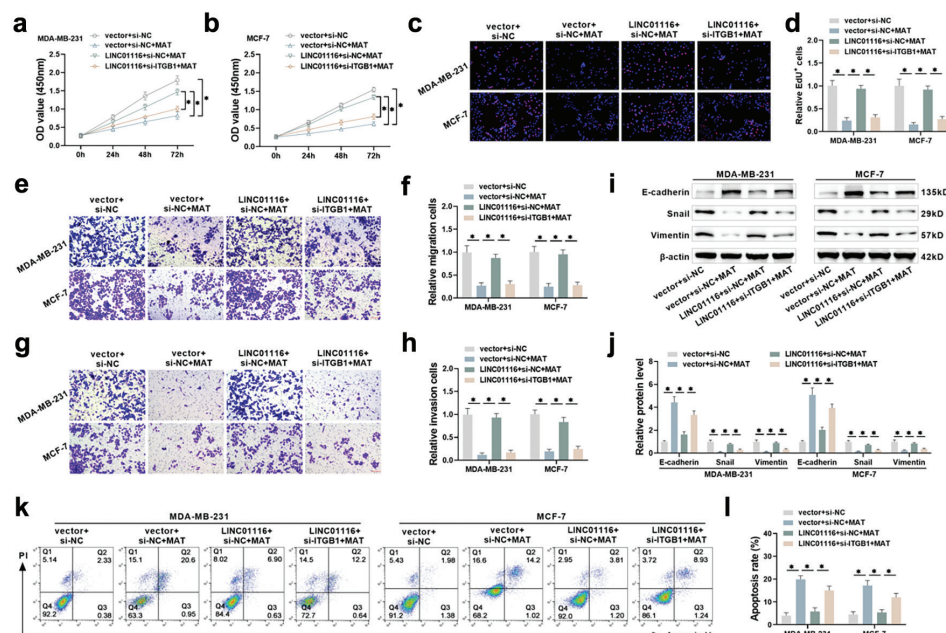


**FIG. 6.** ITGB1 knockdown rescues the attenuated effect of LINC01116 overexpression on the inhibition of BC development by MAT (\*indicates  $p < 0.05$ ). (a, b) si-ITGB1 and/or LINC01116 vectors were transfected into MCF-7 and MDA-MB-231 cells, respectively, and cell proliferation viability was assessed using CCK-8. (c, d) EdU detected BC cell growth. (e, f) Transwell detection of BC cell movement rates. (g, h) Transwell detection of BC cell invasion rates. (i, j) Western blot detected the amounts of EMT-related proteins E-cadherin, snail, and vimentin in two types of BC cells. (k, l) Flow detection of apoptosis in two types of BC cells.

BC, breast cancer; MAT, matrine; EMT, epithelial-mesenchymal transition

pathologic structure of the tumor tissue, which were reversed with LINC01116 overexpression. LINC01116 overexpression also inhibited the reduction and increase of Ki67 and Bax expression, respectively, in tumor tissues following MAT treatment (Figure 7g). This implies that LINC01116 may enhance both malignant BC tumor spread and BC cell proliferation. The qRT-PCR and Western blot analysis revealed that the expression levels of LINC01116, miR-9-5p, and ITGB1 decreased, increased, and decreased, respectively, in BC tumors after MAT administration; the opposite change was observed after LINC01116 overexpression (Figure 7h-j). This finding indicates that MAT inhibits BC tumor growth in vivo via the LINC01116/miR-9-5p/ITGB1 axis.

## DISCUSSION

Comprehensive treatment has become the fundamental premise of tumor treatment, essentially representing the reasonable approach and future development direction of tumor therapy. Patient with BC exhibit a longer survival time, are more sensitive to various treatments, and demonstrate the more typical overall treatment of various malignant tumors.<sup>35</sup> Drug-assisted therapy is now available for patients with BC to improve their survival rate. Traditional Chinese medicine is based on the extensive clinical expertise obtained over thousands of years in China and other Asian nations, and it has exhibited an extraordinary adjuvant therapeutic impact in the treatment of cancer.<sup>7,36</sup> Thus, developing new and

effective Chinese medicinal agents with low side effects is critical for alleviating the negative effects in patients with BC, improving the body's immunity, and increasing the curative rate. MAT offers advantages of clear pharmacological effects, mild therapeutic effects, and excellent safety. Additionally, as a monomer, MAT has a defined chemical structure, which is beneficial for new drug development.<sup>37</sup> In our study, MAT inhibited the proliferative activity of MCF-7 and MDA-MB-231 cells in vitro in a concentration-dependent manner. Furthermore, 8 μm of MAT reduced the OD of the cells by more than half of that of the control cells. Thus, the optimum concentration of MAT for producing a significant effect is 8 μm. The treatment of two BC cell lines with 8 μm of MAT demonstrated a decrease in the number of EdU-positive BC cells, decrease in the number of cells migrating and invading in vitro, and an increase in the rate of apoptosis. These findings demonstrate that MAT could effectively inhibit the biological behaviors of BC cells, which is consistent with the findings of previous studies.<sup>21</sup>

The primary cause of death in patients with BC is tumor metastasis, which refers to the systemic spread of tumor cells.<sup>38</sup> EMT is involved in tumor cell invasion and migration, which is important in the metastasis and dissemination of BC cells.<sup>39,40</sup> Epithelial cells are distinguished by their stable cell-cell junctions, apical-basal polarity, cell-basement membrane interactions, and expression of epithelial marker protein molecules (e.g., E-cadherin). However, transformed mesenchymal cells exhibit fibroblast-like morphology and cellular structure, increased invasive and migratory capacity,

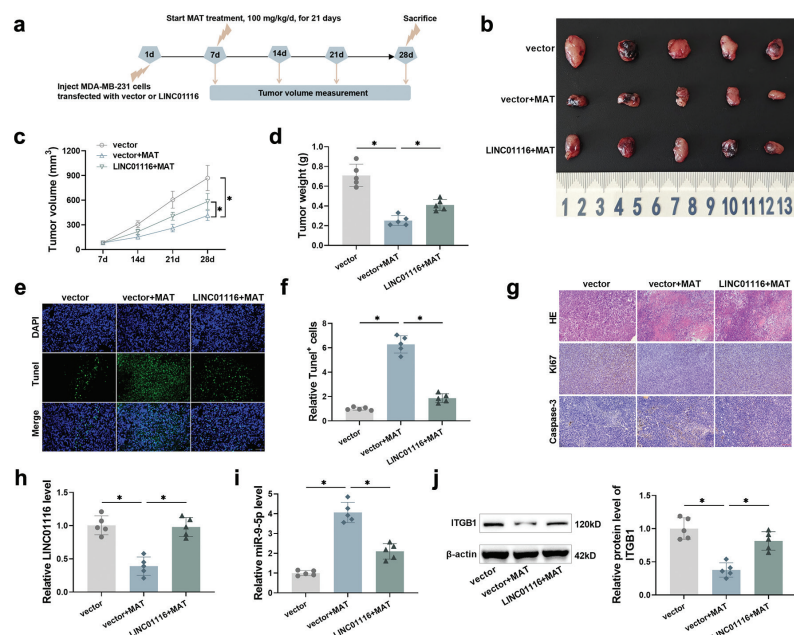


**FIG. 7.** LINC01116 overexpression reduces the anticancer action of MAT on BC development in vivo (\*indicates  $p < 0.05$ ). (a) Timeline for administering naked mice. naked mice were subcutaneously injected with stably transfected vector or LINC01116 overexpressing MDA-MB-231 cells, and MAT was given serially after 7 days (the tumor volume was  $\geq 150 \text{ mm}^3$ ) of breeding until the naked mice were put to death on the 28<sup>th</sup> day. (b) Tumors isolated in vivo after nude mice were killed in each group. (c) Tumor volume changes in naked mice during feeding. (d) Weight of tumors in vivo in naked mice. (e, f) Tunel immunofluorescence staining of tumor tissues. (g) Tumor tissue H & E staining, immunohistochemical staining with Ki67 and Bax. (h, i): qRT-PCR detection of LINC01116 and miR-9-5p expression in tumour tissues. (j) Western blot detected the expression of ITGB1 in tumor tissues. BC, breast cancer; MAT, matrine; H&E, hematoxylin-eosin; qRT-PCR, quantitative real-time polymerase chain reaction.

and increased expression of mesenchymal marker proteins (e.g., Snail and N-cadherin).<sup>41,42</sup> Numerous studies have demonstrated that traditional Chinese medicine and its active components have a stronger inhibitory effect on EMT in the BC cells.<sup>43</sup> In our study, the MCF-7 and MDA-MB-231 cells that were treated with 8 µm of MAT for 24 h exhibited a significant upregulation in E-cadherin expression and downregulation in Snail and N-cadherin expression. This indicates that MAT can successfully suppress the EMT process of BC cells, which is also an essential explanation for the reduced migratory and invasion ability of BC cells.

In recent years, numerous studies have focused on the induction mechanism of EMT, and they have determined that lncRNAs can regulate EMT by interacting with transcriptional regulators.<sup>33,44</sup> The deregulation of lncRNAs plays a significant role in the progression of BC.<sup>45,46</sup> Furthermore, lncRNAs can interact with miRNAs as "sponges" or ceRNAs, reducing the inhibitory effect of miRNAs on mRNAs of downstream target genes.<sup>47</sup> LINC01116 is a lncRNA that is overexpressed in numerous malignant tumors and is essential for cell proliferation, invasion, migration, and apoptosis.<sup>31</sup> Via a database review and experimental assays, we discovered that LINC01116 was significantly overexpressed in BC tissues and cells, and its expression level was significantly reduced after 24 h of treatment with MAT. These findings imply that MAT may inhibit BC cells by impeding the EMT process via the downregulation of LINC01116 expression. To evaluate the probable mechanism of action of LINC01116 dysregulation in BC, we predicted its target miRNA and validated it using the ENCORI database. We discovered that LINC01116 might act as a sponge for miR-9-5p and subsequently determined that the downstream target gene of miR-9-5p was ITGB1. Rescue tests using miR-9-5p overexpression and ITGB1 knockdown demonstrated that LINC01116 upregulated ITGB1 expression by acting as a sponge for miR-9-5p, and MAT mediated the role of the LINC01116/miR-9-5p/ITGB1 axis in BC. In vivo tests revealed that MAT administration at a dose of 100 mg/kg/day significantly reduced the volume and weight of BC tumors in the nude mice model by more than half. Furthermore, the expression levels of LINC01116, miR-9-5p, and ITGB1 in tissues were significantly lower, higher, and lower,

respectively after MAT administration; however, these results were reversed with LINC01116 overexpression. These results were comparable to those of the in vitro cellular experiments. MAT also improved the pathological structure and decreased and increased the Ki67 and Bax expression levels, respectively, in tumor tissues. These findings indicate that MAT might suppress tumor development and metastasis in vivo by modulating the LINC01116/miR-9-5p/ITGB1 axis (Figure 8). MAT has been shown to prevent EMT in BC cells by targeting the downregulation of ITGB1,<sup>48</sup> which is consistent with our study's findings. By defining the upstream gene of ITGB1, we improved the MAT-regulated BC metastatic network and identified new useful targets and approaches for the development of novel drugs and their clinical application.

## CONCLUSION

In this study, we determined the mechanism of action of MAT in BC cell proliferation, EMT, and tumor growth in vivo. We determined that the LINC01116/miR-9-5p/ITGB1 axis may be the primary pathway for the prevention of BC development. Our study's findings may aid in the development of treatments for BC. Traditional surgical treatment is gradually being replaced by a comprehensive treatment approach. In the treatment of tumors, Chinese medicine adjuvant therapy can not only alleviate the symptoms of fatigue, chronic pain, anorexia, and insomnia of patients, but also improve their quality of life and reduce the adverse reactions and complications associated with chemotherapy, radiotherapy, or targeted therapy.<sup>7</sup> MAT adjuvant therapy may improve drug targeting, reduce effects on non-targets, and increase cost-effectiveness. However, the effects of MAT on additional in vivo models have yet to be investigated. Furthermore, given the complex network of BC regulatory pathways, it is uncertain whether MAT can target tumor stem cells to minimize recurrence. Thus, further studies on the effect of MAT on various in vivo induction models are required to validate the anti-BC effect of MAT. Furthermore, the drug's efficacy and safety should be examined via clinical and toxicity testing. Moreover, the dosage of MAT must be optimized and combined with other treatment modalities such

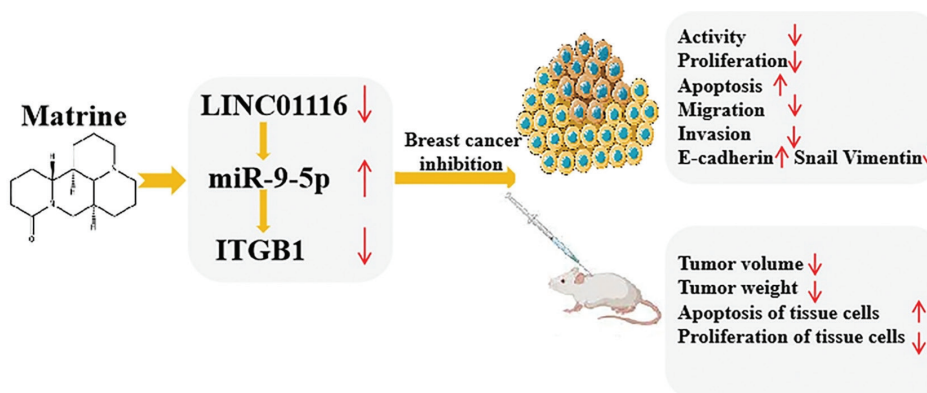


**FIG. 8.** Graphical abstract. Matrine can inhibit the activity, proliferation, migration and invasion of breast cancer cells and intervene in EMT in vitro by regulating the LINC01116/miR-9-5p/ITGB1 axis, also, it can promote apoptosis, and inhibit the growth of tumor cells in vivo by this axis. *EMT, epithelial-mesenchymal transition.*

as chemotherapy, gene therapy, radiotherapy, phototherapy, and immunotherapy, to achieve precise treatment for BC in different patients.

**Ethics Committee Approval:** This study was approved by the Medical Ethics Committee of Zhejiang Cancer Hospital, Hangzhou Institute of Medicine, Chinese Academy of Sciences (approval number: YL-20231023, date: 23.10.2023).

**Informed Consent:** Patient approval has not been obtained as it is performed on animals.

**Data Sharing Statement:** The datasets analyzed during the current study are available from the corresponding author upon reasonable request.

**Authorship Contributions:** Concept- L.R.; Design- L.R.; Materials- Z.F., J.X., X.W., Z.H.; Data Collection or Processing- Z.F., J.X., X.W., Z.H.; Analysis or Interpretation- Y.Z., H.C.; Writing- L.R.

**Conflict of Interest:** The authors declare that they have no conflict of interest.

**Funding:** Zhejiang Province Traditional Chinese Medicine Science and Technology project (project no: 2024ZF037).

## REFERENCES

- Riggio AI, Varley KE, Welm AL. The lingering mysteries of metastatic recurrence in breast cancer. *Br J Cancer*. 2021;124:13-26. [\[CrossRef\]](#)
- Ashrafizadeh M. Cell death mechanisms in human cancers: molecular pathways, therapy resistance and therapeutic perspective. *Journal of Cancer Biomolecules and Therapeutics*. 2024;1:17-40. [\[CrossRef\]](#)
- Rossi L, Mazzara C, Paganini O. Diagnosis and Treatment of breast cancer in young women. *Curr Treat Options Oncol*. 2019;20:86. [\[CrossRef\]](#)
- Tesch ME, Partridge AH. Treatment of breast cancer in young adults. *Am Soc Clin Oncol Educ Book*. 2022;42:1-12. [\[CrossRef\]](#)
- Luo H, Vong CT, Chen H, et al. Naturally occurring anti-cancer compounds: shining from Chinese herbal medicine. *Chin Med*. 2019;14:48. [\[CrossRef\]](#)
- Wang S, Long S, Deng Z, Wu W. Positive role of Chinese herbal medicine in cancer immune regulation. *Am J Chin Med*. 2020;48:1577-1592. [\[CrossRef\]](#)
- Zhang X, Qiu H, Li C, Cai P, Qi F. The positive role of traditional Chinese medicine as an adjunctive therapy for cancer. *Biosci Trend*. 2021;15:283-298. [\[CrossRef\]](#)
- Ho VW, Tan HY, Guo W, et al. Efficacy and safety of Chinese herbal medicine on treatment of breast cancer: a meta-analysis of randomized controlled trials. *Am J Chin Med*. 2021;49:1557-1575. [\[CrossRef\]](#)
- Wang X, Wang C, Guan J, Chen B, Xu L, Chen C. Progress of breast cancer basic research in China. *Int J Biol Sci*. 2021;17:2069-2079. [\[CrossRef\]](#)
- Wang S, Yang S, Yang X, Deng D, Li J, Dong M. Research progress of traditional Chinese medicine monomers in reversing multidrug resistance of breast cancer. *Am J Chin Med*. 2023;51:575-594. [\[CrossRef\]](#)
- Zhao W, Liu J, Li Y, Chen Z, Qi D, Zhang Z. Immune effect of active components of traditional Chinese medicine on triple-negative breast cancer. *Front Pharmacol*. 2021;12:731741. [\[CrossRef\]](#)
- Li X, Tang Z, Wen L, Jiang C, Feng Q. Matrine: A review of its pharmacology, pharmacokinetics, toxicity, clinical application and preparation researches. *J Ethnopharmacol*. 2021;269:113682. [\[CrossRef\]](#)
- Zhang F, Zhang H, Qian W, et al. Matrine exerts antitumor activity in cervical cancer by protective autophagy via the Akt/mTOR pathway in vitro and in vivo. *Oncol Lett*. 2022;23:110. [\[CrossRef\]](#)
- Zhao B, Hui X, Wang J, et al. Matrine suppresses lung cancer metastasis via targeting M2-like tumour-associated-macrophages polarization. *Am J Cancer Res*. 2021;11:4308-4328. [\[CrossRef\]](#)
- Huang Z, Li H, Li Q, Chen X, Liu R, Chang X. Matrine suppresses liver cancer progression and the Warburg effect by regulating the circROBO1/miR-130a-5p/ROBO1 axis. *J Biochem Mol Toxicol*. 2023;37:e23436. [\[CrossRef\]](#)
- Gao Y, Wu C, Huang J, et al. A new strategy to identify ADAM12 and PDGFRB as a novel prognostic biomarker for matrine regulates gastric cancer via high throughput chip mining and computational verification. *Comput Biol Med*. 2023;166:107562. [\[CrossRef\]](#)
- Xu PL, Cheng CS, Jiao JY, Chen H, Chen Z, Li P. Matrine injection inhibits pancreatic cancer growth via modulating carbonic anhydrases: a network pharmacology-based study with in vitro validation. *J Ethnopharmacol*. 2022;287:114691. [\[CrossRef\]](#)
- Feng Z, Sun N, Noor F, et al. Matrine targets BTF3 to inhibit the growth of canine mammary tumor cells. *Int J Mol Sci*. 2023;25:540. [\[CrossRef\]](#)
- Jin J, Fan Z, Long Y, et al. Matrine induces ferroptosis in cervical cancer through activation of piezo1 channel. *Phytomedicine*. 2024;122:155165. [\[CrossRef\]](#)
- Liang X, Ju J. Matrine inhibits ovarian cancer cell viability and promotes apoptosis by regulating the ERK/JNK signaling pathway via p38MAPK. *Oncol Rep*. 2021;45:82. [\[CrossRef\]](#)
- Chen F, Pan Y, Xu J, Liu B, Song H. Research progress of matrine's anticancer activity and its molecular mechanism. *J Ethnopharmacol*. 2022;286:114914. [\[CrossRef\]](#)
- Zhang H, Chen L, Sun X, Yang Q, Wan L, Guo C. Matrine: a promising natural product with various pharmacological activities. *Front Pharmacol*. 2020;11:588. [\[CrossRef\]](#)
- Zhang X, Xu H, Bi X, et al. Src acts as the target of matrine to inhibit the proliferation of cancer cells by regulating phosphorylation signaling pathways. *Cell Death Dis*. 2021;12:931. [\[CrossRef\]](#)
- Hashemi M, Arani HZ, Orouei S, et al. EMT mechanism in breast cancer metastasis and drug resistance: Revisiting molecular interactions and biological functions. *Biomed Pharmacother*. 2022;155:113774. [\[CrossRef\]](#)
- Lüönd F, Sugiyama N, Bill R, et al. Distinct contributions of partial and full EMT to breast cancer malignancy. *Dev Cell*. 2021;56:3203-3221.e11. [\[CrossRef\]](#)
- Park M, Kim D, Ko S, Kim A, Mo K, Yoon H. Breast cancer metastasis: mechanisms and therapeutic implications. *Int J Mol Sci*. 2022;23:6806. [\[CrossRef\]](#)
- Mo RL, Li Z, Zhang P, Sheng MH, Han GC, Sun DQ. Matrine inhibits invasion and migration of gallbladder cancer via regulating the PI3K/AKT signaling pathway. *Naunyn Schmiedebergs Arch Pharmacol*. 2024;397:8129-8143. [\[CrossRef\]](#)
- Huang M, Xin W. Matrine inhibiting pancreatic cells epithelial-mesenchymal transition and invasion through ROS/NF-κB/MMPs pathway. *Life Sci*. 2018;192:55-61. [\[CrossRef\]](#)
- Zhang PP, Zhang F, Zhu K, et al. Matrine exerted an anti-tumor effect on acute myeloid leukemia via the lncRNA LINC01116/miR-592-mediated JAK/STAT pathway inactivation. *Neoplasia*. 2022;69:123-135. [\[CrossRef\]](#)
- Ying H, Jin Y, Guo Y, et al. Long non-coding RNA NUT family member 2A-antisense RNA 1 sponges microRNA-613 to increase the resistance of gastric cancer cells to matrine through regulating oxidative stress and vascular endothelial growth factor A. *Aging (Albany NY)*. 2022;14:5153-5162. [\[CrossRef\]](#)
- Xu Y, Yu X, Zhang M, et al. Promising advances in LINC01116 related to cancer. *Front Cell Dev Biol*. 2021;9:736927. [\[CrossRef\]](#)
- Fang X, Ren LH, Shrestha SM, et al. LINC01116 modulates EMT process via binding with AGO1 mRNA in oesophageal squamous cell carcinoma. *Biochim Biophys Acta Mol Cell Res*. 2023;1870:119447. [\[CrossRef\]](#)
- Tao H, Zhang Y, Yuan T, et al. Identification of an EMT-related lncRNA signature and LINC01116 as an immune-related oncogene in hepatocellular carcinoma. *Aging (Albany NY)*. 2022;14:1473-1491. [\[CrossRef\]](#)
- Zhou J, Jiang YY, Chen H, Wu YC, Zhang L. Tanshinone I attenuates the malignant biological properties of ovarian cancer by inducing apoptosis and autophagy via the inactivation of PI3K/AKT/mTOR pathway. *Cell Prolif*. 2020;53:e12739. [\[CrossRef\]](#)
- Trayes KP, Cokenakes SEH. Breast cancer treatment. *Am Fam Physician*. 2021;104:171-178. [\[CrossRef\]](#)
- Wang Z, Qi F, Cui Y, et al. An update on Chinese herbal medicines as adjuvant treatment of anticancer therapeutics. *Biosci Trends*. 2018;12:220-239. [\[CrossRef\]](#)
- Sun XY, Jia LY, Rong Z, et al. Research Advances on Matrine. *Front Chem*. 2022;10:867318. [\[CrossRef\]](#)
- Liu YM, Ge JY, Chen YF, et al. Combined single-cell and spatial transcriptomics reveal the metabolic evolution of breast cancer during early dissemination. *Adv Sci (Weinh)*. 2023;10:e2205395. [\[CrossRef\]](#)
- Huang Y, Hong W, Wei X. The molecular mechanisms and therapeutic strategies of EMT in tumor progression and metastasis. *J Hematol Oncol*. 2022;15:129. [\[CrossRef\]](#)
- Yang J, Antin P, Berx G, et al. EMT International Association (TEMTIA). Guidelines and definitions for research on epithelial-mesenchymal transition. *Nat Rev Mol Cell Biol*. 2020;21:341-352. [\[CrossRef\]](#)
- Lambert AW, Weinberg RA. Linking EMT programmes to normal and neoplastic epithelial stem cells. *Nat Rev Cancer*. 2021;21:325-338. [\[CrossRef\]](#)

42. Marconi GD, Fonticoli L, Rajan TS, et al. Epithelial-mesenchymal transition (EMT): the Type-2 EMT in wound healing, tissue regeneration and organ fibrosis. *Cells*. 2021;10:1587. [\[CrossRef\]](#)
43. Lu Y, Ding Y, Wei J, et al. Anticancer effects of Traditional Chinese Medicine on epithelial-mesenchymal transition EMT in breast cancer: Cellular and molecular targets. *Eur J Pharmacol.* 2021;907:174275. [\[CrossRef\]](#)
44. McCabe EM, Rasmussen TP. lncRNA involvement in cancer stem cell function and epithelial-mesenchymal transitions. *Semin Cancer Biol.* 2021;75:38-48. [\[CrossRef\]](#)
45. Shen X, Zhong J, Yu P, Zhao Q, Huang T. YY1-regulated LINC00152 promotes triple negative breast cancer progression by affecting on stability of PTEN protein. *Biochem Biophys Res Commun.* 2019;509:448-454. [\[CrossRef\]](#)
46. Zheng L, Zhang Y, Fu Y, et al. Long non-coding RNA MALAT1 regulates BLCAP mRNA expression through binding to miR-339-5p and promotes poor prognosis in breast cancer. *Biosci Rep.* 2019;39:BSR20181284. [\[CrossRef\]](#)
47. Zuo Y, Li Y, Zhou Z, Ma M, Fu K. Long non-coding RNA MALAT1 promotes proliferation and invasion via targeting miR-129-5p in triple-negative breast cancer. *Biomed Pharmacother.* 2017;95:922-928. [\[CrossRef\]](#)
48. Ren L, Mo W, Wang L, Wang X. Matrine suppresses breast cancer metastasis by targeting ITGB1 and inhibiting epithelial-to-mesenchymal transition. *Exp Ther Med.* 2020;19:367-374. [\[CrossRef\]](#)